Galerkin Boundary Integral Analysis for the 3D Helmholtz Equation

M. R. Swager[1], L. J. Gray[2], and S. Nintcheu Fata[2]

Abstract: A linear element Galerkin boundary integral analysis for the three-dimensional Helmholtz equation is presented. The emphasis is on solving acoustic scattering by an open (crack) surface, and to this end both a dual equation formulation and a symmetric hypersingular formulation have been developed. All singular integrals are defined and evaluated via a boundary limit process, facilitating the evaluation of the (finite) hypersingular Galerkin integral. This limit process is also the basis for the algorithm for post-processing of the surface gradient. The analytic integrations required by the limit process are carried out by employing a Taylor series expansion for the exponential factor in the Helmholtz fundamental solutions. For the open surface, the implementations are validated by comparing the numerical results obtained by using the two methods.

Keywords: Helmholtz equation, boundary integral method, Galerkin approximation, hypersingular integrals

1 Introduction

The application of boundary integral equations for the solution of acoustic wave scattering and transmission problems has been discussed extensively in the literature, see for example Wu and Wan (1992); Hwang (1997a,b); Yang (2000) and additional articles referenced below. As is well known, one of the attractions of the integral equation formulation is its suitability for scattering from finite bodies in an infinite domain: with this approach an artificial truncation of the domain is avoided, and the Green's function automatically incorporates the boundary condition at infinity. Moreover, as the calculation only involves the surface of the scatterer, a likely additional benefit is a reduction in problem size and computational effort.

[1] Department of Mathematics, Emporia State University, Emporia KS 66801.
[2] Computer Science and Mathematics Division,Oak Ridge National Laboratory, Oak Ridge, TN 37831 USA.

The velocity potential $\phi(x,y,z)$ for a time harmonic acoustic wave with frequency ω satisfies the Helmholtz equation

$$\nabla^2\phi + k^2\phi = 0 \,, \tag{1}$$

in the domain $\mathscr{D}$, where $k = \omega/c$ is the wave number, c the speed of sound of the medium. The corresponding boundary integral equation is usually written as Martin (2006)

$$\phi(P) + \int_\Sigma \left\{ \phi(Q)\frac{\partial G}{\partial \mathbf{n}}(P,Q) - G(P,Q)\frac{\partial \phi}{\partial \mathbf{n}}(Q) \right\} dQ = 0 \qquad P \in \mathscr{D} \,, \tag{2}$$

where $\mathbf{n} = \mathbf{n}(Q)$ denotes the unit outward normal on the boundary Σ of $\mathscr{D}$, and it has been assumed that P is a point *interior* to $\mathscr{D}$. For our purposes it is slightly more convenient to use an exterior limit in which case for P *exterior* to $\mathscr{D}$, one can write

$$\mathscr{P}(P) \equiv \int_\Sigma \left\{ \phi(Q)\frac{\partial G}{\partial \mathbf{n}}(P,Q) - G(P,Q)\frac{\partial \phi}{\partial \mathbf{n}}(Q) \right\} dQ = 0 \qquad P \notin \mathscr{D} \cup \Sigma \,. \tag{3}$$

In the above, $\mathbf{R} = Q - P$, $r = \|\mathbf{R}\|$, and the (non-normalized) free-space Green's function $G(P,Q)$ can be taken as Kleinman and Roach (1974)

$$G(P,Q) = \frac{e^{ikr}}{r} \,. \tag{4}$$

A 'boundary only' statement, for either the interior or exterior equation, can then be achieved by considering the limit as P approaches the boundary, and the resulting singular integrals (at $Q = P$) are defined and evaluated in terms of this limit Gray, Glaeser, and Kaplan (2004). Note that the exterior boundary limit allows the non-standard normalization of the Green's function in Eq. (4), as the standard normalization is only required in order to get the correct coefficient for the free term ($\phi(P)$). The two boundary equations are of course identical, the exterior limit evaluation will produce a term to balance the free term that is present in Eq. (2).

The boundary limit formulation will be important for analyzing the corresponding derivative (hypersingular) equation

$$\mathscr{F}(P) \equiv \int_\Sigma \left\{ \phi(Q)\frac{\partial^2 G}{\partial \mathbf{N}\partial \mathbf{n}}(P,Q) - \frac{\partial G}{\partial \mathbf{N}}(P,Q)\frac{\partial \phi}{\partial \mathbf{n}}(Q) \right\} dQ = 0 \,, \tag{5}$$

where $\mathbf{N} = \mathbf{N}(P)$ is again the unit outward normal. In general, the hypersingular equation is essential for symmetric formulations Bonnet, Maier, and Polizzotto (1998) and for dealing with crack geometries Cruse (1988), *e.g.*, the scattering from

thin objects Wu and Wan (1992); Hwang (1997b) in acoustics. However, this velocity equation plays an even larger role for acoustics, in that it is a key component of the well known method of Burton and Miller (1971) for handling irregular frequencies (see also Qian, Han, and Atluri (2004)). Considering its importance, and as well the difficulties in dealing with hypersingular integrals via collocation Martin and Rizzo (1989), it is not surprising that much attention has been paid to this issue. Various hypersingular schemes for acoustics have been developed, including several methods for manipulating Eq. (5) so as to completely avoid the hypersingularity Qian, Han, and Atluri (2004); Chien, Rajiyah, and Atluri (1990); Qian, Han, Ufimtsev, and Atluri (2004); Wu, Seybert, and Wan (1991).

An opposite approach is taken in this paper: the hypersingular integrals, in Galerkin form, are evaluated based upon the direct algorithms developed in Gray, Glaeser, and Kaplan (2004); Gray, Salvadori, Phan, and Mantič (2006). These methods do not employ any regularization or reformulation of the integral, and standard continuous elements can be used. Moreover, in this direct formulation the hypersingular integral is seen to be finite (though the component coincident and edge-adjacent singular integrals are separately divergent), and thus there is no need to invoke the Hadamard Finite Part methodology Ioakimidis (1982). One goal of this paper is to show that the limit techniques are easily applicable and are effective for implementing Eq. (3) and Eq. (5). As a demonstration, the derivative equation is employed to solve for the scattering from crack surfaces.

As is well known Cruse (1988), the boundary integral equation for surface potential, Eq. (3), is the same on either side of the crack, and thus a crack geometry cannot be solved by employing this equation alone. There are two main techniques for overcoming this degeneracy, both, by necessity, invoking the hypersingular velocity equation, Eq. (5). In a 'dual equation' formulation Gray (1989); Hong and Chen (1988); Portela (1993), both Eq. (3) and Eq. (5) are employed on the crack surface and the potential and normal velocity on the sides of the crack are explicit in the formulation. In the second Bui (1977); Frangi (1998), only Eq. (5) is written on the crack, and in this case the crack surface variables are the jump in potential $[\phi] = \phi^+ - \phi^-$ and normal velocity $[\phi_{,\mathbf{n}}] = \phi_{,\mathbf{n}}^+ + \phi_{,\mathbf{n}}^-$. If needed, the separate potentials and velocities on the crack surfaces can be obtained in a post-processing step. The two algorithms are developed herein, and by comparing results, both implementations can be validated.

Although much of the previous boundary integral work for the Helmholtz equation has employed a collocation approximation, Galerkin methods have become more commonplace Qian, Han, and Atluri (2004); von Estorff, Rjasanow, Stolper, and Zaleski (2005); Polimeridis and Yioultsis (2008). The next section presents the Galerkin implementation for Eq. (3) and Eq. (5), in the context of a linear element

approximation. The post-processing of the surface gradient is discussed in Section 3, while the two crack algorithms are discussed in Section 4.

2   Galerkin Formulation

2.1   Linear Interpolation

For purposes of discussion it suffices to employ a linear element, as the treatment of higher order interpolations can be based upon this analysis Sutradhar, Paulino, and Gray (2008). As in Gray, Glaeser, and Kaplan (2004), it is convenient to use an equilateral triangle parameter space $\{\eta, \xi\}$, where $-1 \leq \eta \leq 1$ and $0 \leq \xi \leq \sqrt{3}(1 - |\eta|)$. The linear shape functions are

$$
\begin{aligned}
\psi_1(\eta, \xi) &= \frac{\sqrt{3}(1 - \eta) - \xi}{2\sqrt{3}} \\
\psi_2(\eta, \xi) &= \frac{\sqrt{3}(1 + \eta) - \xi}{2\sqrt{3}} \\
\psi_3(\eta, \xi) &= \frac{\xi}{\sqrt{3}},
\end{aligned}
\tag{6}
$$

and for an element defined by the three vertices $\{Q_j = (x_j, y_j, z_j)\}$, the corresponding isoparametric approximations of the surface and surface functions are

$$
\begin{aligned}
\Sigma(\eta, \xi) &= \sum_{j=1}^{3} (x_j, y_j, z_j) \psi_j(\eta, \xi) \\
\phi(\eta, \xi) &= \sum_{j=1}^{3} \phi(Q_j) \psi_j(\eta, \xi) \\
\phi_{,\mathbf{n}}(\eta, \xi) &= \sum_{j=1}^{3} \phi_{,\mathbf{n}}(Q_j) \psi_j(\eta, \xi),
\end{aligned}
\tag{7}
$$

where $\phi_{,\mathbf{n}} = \partial \phi / \partial \mathbf{n}$.

The Galerkin approximation of Eq. (3) and Eq. (5) can then be defined as

$$
\begin{aligned}
\int_{\Sigma} \hat{\psi}_k(P) \mathscr{P}(P) \, dP &= 0 \\
\int_{\Sigma} \hat{\psi}_k(P) \mathscr{F}(P) \, dP &= 0
\end{aligned}
\tag{8}
$$

where the weight function $\hat{\psi}_k(P)$ consists of all shape functions $\psi_l(P)$ that are nonzero at a particular node P_k. The weight function $\hat{\psi}_k(P)$ therefore has limited support, being non-zero only on the elements containing P_k.

2.2   Singular Integration

In addition to the Green's function, Eq. (4), the kernel functions that appear in Eq. (8) are

$$
\begin{aligned}
\frac{\partial G}{\partial n} &= -\frac{e^{ikr}}{r^3}\mathbf{n}\cdot\mathbf{R}(1-ikr) \\
\frac{\partial G}{\partial N} &= \frac{e^{ikr}}{r^3}\mathbf{N}\cdot\mathbf{R}(1-ikr) \\
\frac{\partial^2 G}{\partial N\partial n} &= (\mathbf{N}\cdot\mathbf{R})(\mathbf{n}\cdot\mathbf{R})\frac{e^{ikr}}{r^5}\left(k^2r^2+3ikr-3\right)+(\mathbf{N}\cdot\mathbf{n})\frac{e^{ikr}}{r^3}(1-ikr)\,.
\end{aligned}
\tag{9}
$$

As noted above, Eq. (3) and Eq. (5) are strictly defined only for a point P_E exterior to the domain. The boundary integral statements are obtained by taking the limit as P_E approaches the boundary, in the form $P_E = P + \varepsilon\mathbf{N}$, $\varepsilon \to 0$. The singular ($Q = P$) integrals are therefore defined in terms of this limit, and the chief task, most especially for the hypersingular kernel, is to evaluate this boundary limit.

The singular integration algorithms for the most part follow the procedures described in Gray, Glaeser, and Kaplan (2004) for the Laplace equation. The discussion herein will therefore focus solely on the treatment of the one additional complicating factor in the Helmholtz kernels, namely the presence of the exponential. Although the analytic integrations required to carry out the boundary limit are (as in the Laplace case) no longer immediately possible, it is a simple matter to employ suitable Taylor expansions to split all integrals into a singular term that can be integrated analytically, plus a completely nonsingular remainder that can be safely handled numerically.

The implementation of Eq. (8) departs from that in Gray, Glaeser, and Kaplan (2004); Sutradhar, Paulino, and Gray (2008) solely in one detail, the evaluation of the singular integrals involving the Green's function. For these integrals we follow Polimeridis and Yioultsis (2008) and note that no splitting of the integrand is necessary: after the transformation to polar coordinates, the r denominator in the Green's function is eliminated and the remaining exponential can be integrated exactly. Compared to employing the Taylor expansion, this provides a bit more accuracy, and also simplifies the implementation.

It suffices to describe the Taylor expansion procedure for the hypersingular kernel

$$
\begin{aligned}
\frac{\partial^2 G}{\partial N\partial n} &= e^{ikr}\mathcal{W}(Q,P) \\
\mathcal{W}(Q,P) &= \left\{\frac{(\mathbf{N}\cdot\mathbf{R})(\mathbf{n}\cdot\mathbf{R})}{r^5}\left(k^2r^2+3ikr-3\right)+\frac{\mathbf{N}\cdot\mathbf{n}}{r^3}(1-ikr)\right\}
\end{aligned}
\tag{10}
$$

as the first derivative kernels can be handled in a similar fashion. To split the integral we simply write

$$
e^{ikr} = 1 + ikr - \frac{k^2 r^2}{2} + \left\{ e^{ikr} - (1 + ikr - \frac{k^2 r^2}{2}) \right\} , \tag{11}
$$

resulting in a singular kernel

$$
\mathscr{W}(Q,P) \left\{ 1 + ikr - \frac{k^2 r^2}{2} \right\} \tag{12}
$$

and the nonsingular remainder function

$$
\mathscr{W}(Q,P) \left\{ e^{ikr} - 1 - ikr + \frac{k^2 r^2}{2} \right\} . \tag{13}
$$

The required analytic integration and limit evaluation are easily automated using a symbolic computation program, *e.g.*, Maple or Mathematica. Note too that there are nonsingular terms contained in the singular term that could be split off and treated numerically; it is simply a matter of choice and convenience as to how these terms are handled. In this work, the entire singular term is handled with the partial analytic integration methods. For the coincident singular integral, either two Gray, Glaeser, and Kaplan (2004) or three Gray, Salvadori, Phan, and Mantič (2006) dimensions of the four dimensional parameter space integral can be evaluated analytically. For the edge and vertex singular integrals, one analytic integration suffices, but two can be carried out for the edge integral.

A two term expansion has been employed so that the remainder in Eq. (11) is $\mathscr{O}(r^3)$. As the hypersingular kernel W(Q,P) is $\mathscr{O}(r^{-3})$, the numerically evaluated remainder function in Eq. (13) is finite at $r = 0$. Thus, in the evaluation of the coincident integral, when $r = 0$ occurs the expression for the kernel can be replaced by the correct limiting value.

Clearly, there is no unique way of accomplishing the splitting, one can of course choose to employ further terms in the Taylor expansion. Thus, in this work the two term expansion has also been employed (solely for consistency) for the first derivative kernels, whereas a one-term expansion would have sufficed. The price that is paid for including more terms is that the analytic expressions become lengthier.

A critical aspect in the analysis of the hypersingular kernel is to establish the existence of the limit. The coincident and adjacent edge integrals are in fact separately divergent, of the form $\log(\varepsilon^2)$, and these terms must be identified and shown to cancel. The Helmholtz equation is, however, covered by the proof for Laplace

equation Gray, Glaeser, and Kaplan (2004). The most singular terms in Eq. (9) are for $k = 0$, and for the hypersingular kernel this results in

$$\frac{\mathbf{N} \cdot \mathbf{n}}{r^3} - 3\frac{(\mathbf{N} \cdot \mathbf{R})(\mathbf{n} \cdot \mathbf{R})}{r^5} \ . \tag{14}$$

This, not surprisingly, is precisely the second derivative Laplace kernel, and thus, the divergent terms in the Helmholtz integrals are exactly the same as for Laplace. The boundary limit definition and algorithm therefore provides an alternative to the commonly employ Hadamard Finite Part Ioakimidis (1982) approach to the evaluation of the hypersingular integral.

2.3   Code validation

This section presents some simple calculations aimed at demonstrating that the implementations for the potential and velocity equations are correct. The problem boundary is the unit sphere, and both interior Dirichlet and exterior Neumann problems are solved. For the interior problem, the potential boundary conditions are taken from a point source

$$\phi(Q) = G(P_E, Q) = \frac{\mathrm{e}^{ikr}}{r} \ , \tag{15}$$

and the exterior point P_E is either $(2,0,0)$ or $(1.5,0,0)$. The exact value of surface velocity is then given by Eq. (9)

$$\frac{\partial \phi}{\partial n}(Q) = \frac{\partial G}{\partial n}(P_E, Q) = -\frac{e^{ikr}}{r^3}\mathbf{n} \cdot \mathbf{R}(1 - ikr) \ . \tag{16}$$

The value of k was chosen to be 1, 2 or 3, and the reported error is the point-wise $\mathscr{L}_2$ error

$$\left(\frac{1}{M}\sum_{j=1}^{M}|\varepsilon_j|^2\right)^{1/2} \tag{17}$$

where M is the number of nodes and ε_j is the nodal error.

For the exterior Neumann problem, the source is located at the exterior points (now inside the sphere) $(0,0,0)$ and $(0,0,0.5)$, and the roles of surface potential and flux are reversed.

Figures 1 and 2 display the errors when the interior and exterior problems are solved using the potential equation, respectively. Three different meshes are employed for the sphere, 80, 512 and 2048 elements (having 42, 258, and 1026 nodes, respectively), and the logarithm of the error is plotted as a function of the logarithm of the
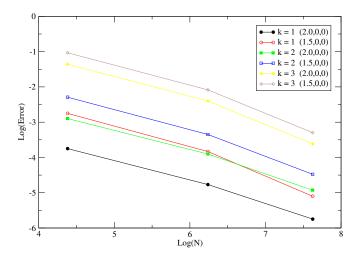
Figure 1: The log of the $\mathscr{L}_2$ error plotted versus the log of the number of elements, for the interior Dirichlet problem solved using the potential equation.

Table 1: Convergence rates for the interior Dirichlet problem.

	$k=1$		$k=2$		$k=3$	
	$(2,0,0)$	$(1.5,0,0)$	$(2,0,0)$	$(1.5,0,0)$	$(2,0,0)$	$(1.5,0,0)$
$\mathscr{P}$	-0.629	-0.722	-0.682	-0.707	-0.662	-0.663
$\mathscr{F}$	-0.675	-0.645	-0.826	-0.755	-0.778	-0.762

number of elements. As expected, the errors increase with higher frequency, and are larger when the source is closer to the sphere boundary. Also as appropriate, the errors decrease with mesh size.

Figures 3 and 4 report the corresponding results when the potential equation is replaced by the hypersingular velocity equation. Except for the exterior Neumann calculations with wave number $k = 1$, these results are consistent with the results from the potential equation (see the discussion below).

If it is assumed that the $\mathscr{L}_2$ error is of the form AN_E^{α}, where N_E is the number of elements, then a least squares fit to the curves in the above figures gives an estimate of the convergence rate α. These values are reported in Table 1 and Table 2 for the interior and exterior problems, respectively. Although three data points stopping
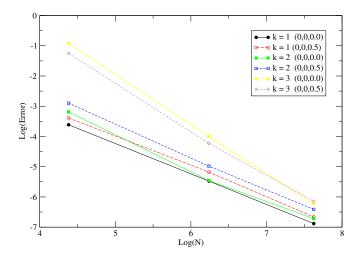
Figure 2: The log of the $\mathscr{L}_2$ error plotted versus the log of the number of elements, for the exterior Neumann problem solved using the potential equation.
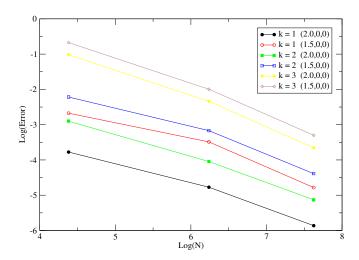

Figure 3: The log of the $\mathscr{L}_2$ error plotted versus the log of the number of elements, for the interior Dirichlet problem solved using the velocity equation.
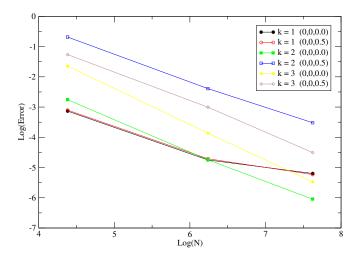
Figure 4: The log of the $\mathscr{L}_2$ error plotted versus the log of the number of elements, for the exterior Neumann problem solved using the velocity equation.

Table 2: Convergence rates for the exterior Neumann problem.

Source	$k=1$		$k=2$		$k=3$	
	$(0,0,0)$	$(0,0,0.5)$	$(0,0,0)$	$(0,0,0.5)$	$(0,0,0)$	$(0,0,0.5)$
$\mathscr{P}$	-0.971	-0.982	-0.875	-0.929	-0.720	-0.828
$\mathscr{F}$	–	–	-1.000	-0.724	-1.012	-0.928

at $N_E = 2048$ is admittedly too few to draw any firm conclusions, the numbers in these tables are reasonably consistent (with one exception discussed below). Noting that $h^{-2} \approx N_E$, h the mesh size, then the convergence for the exterior Neumann problem is roughly quadratic, $\mathscr{L}_2 = \mathscr{O}(h^2)$, as expected. For the interior Dirichlet problem the numbers are close to 0.75, which is the the expected convergence rate $\mathscr{L}_2 = \mathscr{O}(h^{3/2})$ Fata and Gray (2009).

The exception is the exterior calculation for the lowest frequency $k = 1$ solved with the flux equation; the error for the calculation with 2048 elements, while accurate, is nevertheless out of line with the less refined meshes. The fact that this happens for both source point locations, and that the corresponding calculations for $k = 2$ and $k = 3$ show reasonable convergence rates, may indicate that $k = 1$ is close to an

Table 3: $\mathscr{L}_2$ errors in computed potential for the exterior Neumann problem, $k = 1$, using the flux equation alone (F), and a linear combination (LC) of the integral equations.

	$P = (0,0,0)$		$P = (0,0,0.5)$	
N_E	F	LC	F	LC
80	0.02094	0.02444	0.03844	0.03328
512	0.00374	0.00422	0.00662	0.00611
2048	0.00472	0.00139	0.00467	0.00166

irregular frequency for the flux equation. This possibility is supported by the results in Table 3. For $k = 1$ and the exterior Neumann problem on the sphere, this table lists the $\mathscr{L}_2$ errors obtained using the flux equation, along with the errors when the solution is obtained from a 'Burton-Miller' linear combination of potential (coefficient 1) and flux (coefficient $i/4$) equations Burton and Miller (1971). For the linear combination, the errors for the 2048 element calculations now show the expected convergence, suggesting that $k = 1$ may be close to an irregular frequency.

3   Surface Velocity

Once the boundary integral equation is solved, ϕ and $\phi_{,\mathbf{n}}$ on the boundary are known functions. However, for some applications, knowledge of the normal derivative does not suffice, the surface velocity vector $\nabla\phi$ is required. The post-processing evaluation of these derivatives can be based upon a gradient boundary integral equation, one similar to Eq. (5),

$$\nabla\phi(P_I) = \int_\Sigma \left\{ \nabla G(P_I, Q) \frac{\partial\phi}{\partial\mathbf{n}}(Q) - \phi(Q)\nabla\frac{\partial G}{\partial\mathbf{n}}(P_I, Q) \right\} \mathrm{d}Q. \tag{18}$$

Here the P_I is used to emphasize that an interior limit is now employed, in order to have the gradient term that appears on the left hand side. Were it not for the presence of the hypersingular kernel, implementing this equation would be easy and straightforward, requiring little discussion. As it is, the difficulties presented by this kernel have given rise to a variety of proposed algorithms for surface gradient (in elasticity, surface stress) evaluation (see for example Schwab and Wendland (1999); Graciani, Mantič, Paris, and Cañas (2000); Okada, Rajiyah, and Atluri (1989); Zhao and Lan (1999).

Not surprisingly, the boundary limit definition and the related (hyper)singular integration algorithms can be exploited to develop an accurate gradient method based

Table 4: Maximum $\mathscr{L}_2$ errors for the gradient components when solving the exterior Neumann problem using the potential equation.

N_E	$k = 1$		$k = 2$		$k = 3$	
	$(0,0,0)$	$(0,0,0.5)$	$(0,0,0)$	$(0,0,0.5)$	$(0,0,0)$	$(0,0,0.5)$
80	0.0278	0.0644	0.0455	0.1365	0.0724	0.2220
512	0.0119	0.0187	0.0190	0.0323	0.0277	0.0534
2048	0.0042	0.0057	0.0067	0.0094	0.0097	0.0149

upon direct evaluation of the hypersingular terms. Moreover, as discussed in detail in Gray, Phan, and Kaplan (2004), and summarized below, the limit definition leads to a highly efficient scheme that avoids a complete boundary integration; in fact, the calculation is limited to the singular integrals. This section will demonstrate the effectiveness of this method when applied to the Helmholtz equation. Moreover, in Gray, Phan, and Kaplan (2004), the gradient algorithm was described in the context of the $3D$ Laplace equation; the Helmholtz implementation is then especially easy, as it is precisely the same algorithm as for Laplace. This is discussed further below.

The simple but effective idea proposed in Gray, Phan, and Kaplan (2004) is to also write the exterior gradient equation

$$0 = \int_{\Sigma} \left\{ \nabla G(P_E, Q) \frac{\partial \phi}{\partial \mathbf{n}}(Q) - \phi(Q) \nabla \frac{\partial G}{\partial \mathbf{n}}(P_E, Q) \right\} \mathrm{d}Q \,, \tag{19}$$

and then take the difference of the two equations. As there is no free term in the exterior equation, the gradient quantity in Eq. (18) is untouched by subtracting the two equations. Moreover, on the right hand side only the singular integrals that are discontinuous crossing the boundary survive the differencing: the boundary integration is therefore reduced to local (to P) contributions, and indeed much of the singular integration is continuous across the boundary and disappears. An additional benefit is that all of the terms that do remain can be integrated (partially) analytically. Further details can be found in Gray, Phan, and Kaplan (2004).

For the Helmholtz equation, the nonsingular integrals involving the remainder from the Taylor expansion immediately vanish. Moreover, as with the divergent terms in the hypersingular integral, and for essentially the same reason, the Helmholtz gradient analysis will yield precisely the same formulas as for the Laplace equation. Only the leading order singular terms contribute, and the Laplace and Helmholtz kernel functions are, modulo less singular terms, just $1/r$ and its derivatives. The two algorithms are therefore the same, the only difference being the input boundary values of ϕ and $\phi_{,\mathbf{n}}$.

Table 5: Maximum $\mathscr{L}_2$ errors for the gradient components when solving the interior Dirichlet problem using the velocity equation.

N_E	$k = 1$		$k = 2$		$k = 3$	
	$(0,0,0)$	$(2.0,0,0)$	$(1.5,0,0)$	$(0,0,0.5)$	$(0,0,0)$	$(0,0,0.5)$
80	0.0564	0.0742	0.1164	0.3884	0.3135	0.6473
512	0.0080	0.0377	0.0212	0.0535	0.0730	0.1155
2048	0.0031	0.0092	0.0071	0.0141	0.0207	0.0315

Table 4 displays the maximum (over the three gradient components) $\mathscr{L}_2$ error, based upon the solution of the exterior Neumann problem using the potential equation. Table 5 shows the corresponding results for the interior Dirichlet problem solved with the velocity equation. In both calculations the convergence is better than linear but not quite quadratic.

4   Open surfaces

A crack can be viewed as a thin inclusion for which the thickness is idealized as zero. This 'open surface' therefore has two sides, with separate values of potential and normal derivative on each side. As the boundary conditions supply two of these four values, there are two unknowns for each point on the idealized crack surface. The exception is for points on the crack front, where the potentials must be equal.

As is well known Cruse (1988), a standard potential equation formulation fails for a crack geometry: this equation is identical on both sides of the crack, and therefore it does not provide a sufficient number of independent equations. An effective boundary integral fracture algorithm therefore requires the use of the hypersingular equation, and there are two basic ways to do this. One technique is based upon the observation that the hypersingular equation, integrated over both sides of the crack, is equivalent to integrating over one side with the jump variables Bui (1977); Maier, Novati, and Cen (1995); Frangi (1998)

$$[\phi](P) = \phi(P^+) - \phi(P^-) \tag{20}$$
$$[\phi_{,\mathbf{n}}] = \phi_{,\mathbf{n}}(P^+) + \phi_{,\mathbf{n}}(P^-).$$

The Cauchy Principal value integral of the kernel $\partial G / \partial N$ involves the difference of the fluxes rather than the sum, but as the usual boundary condition is specified normal derivative, this term can be incorporated into the known right hand side. After the jump in potential is solved for, the individual potential values, if needed, can be computed in a post-processing step using the potential equation. In this equation

it is again only the Cauchy Principal value contribution that is not a function of the jump in potential $[\phi]$, due to the discontinuity crossing the boundary it depends upon the sum of potentials. However by rewriting the sum as

$$\phi(P^+) + \phi(P^-) = 2\phi(P^+) - \left(\phi(P^+) - \phi(P^-)\right) , \tag{21}$$

the last term on the right is a known quantity, and the unknowns are solely the potentials on the $+$ side of the crack. Moreover, as only the CPV integrals enter into the coefficient matrix, the system is sparse. Note that the $+$ and $-$ sides of the crack are determined by the orientation of the normal vector. As an exterior normal has been assumed, this vector must point into 'the gap' between the two surfaces. Consequently, if the normal vectors on the elements are reversed, the two sides of the crack switch appropriately.

The method of 'dual equations', as the name implies, employs both equations on the crack Gray (1989); Hong and Chen (1988); Portela (1993). Note that for elements having an edge along the crack front, the hypersingular integral, even in Galerkin form, is not finite: logarithmic singularities along this edge do not vanish Gray, Glaeser, and Kaplan (2004). Thus, in both methods, the hypersingular equation for a crack front node is replaced by the condition $[\phi] = 0$.

In most cases, it is preferable to use the first approach as this is computationally more efficient, and with a Galerkin approximation, a symmetric system of equations can be generated. Even if the post-processing step is needed this approach should outperform the dual equation method, due to the larger system of equations being solved. There are however situations where the dual equation formulation is essential, as it provides a system of equations explicitly relating all values of potential and flux. This would be the case if Robin type boundary conditions are given on the crack surface.

The two test problems will be solved using both methods. The agreement of the two solutions will validate the crack algorithms and the post-processing, and moreover provide additional evidence that the implementations of the two equations are correct. In the first set of calculations, the crack surface is the unit disk $x^2 + y^2 \leq 1$ in the $z = 0$ plane, and the prescribed boundary condition is $\phi_{,\mathbf{n}} = 1$ on both sides of the disk. Table 6 lists the L_2 norm of the difference in the computed potential on the $+$ of the crack: in this case the jump in potential is identically zero, so the $-$ side is identical. The differences in the direct (dual equation) and the post-processing solutions are seen to be independent of k and decay with refined mesh, good indications that the implementations are correct.

A final example involves a curved boundary and sharply different potential solutions on the two sides of the crack. A mesh for the unit sphere (512 elements and 258 nodes) was converted to an open surface by removing one element. As above,

Table 6: Difference, in L_2 norm, between the dual equation potential solution and the post-processed hypersingular solution for the disk crack.

N	$k = 1$	$k = 2$	$k = 3$
149	1.670(-4)	1.669(-4)	1.668(-4)
263	1.066(-4)	1.067(-4)	1.067(-4)
350	8.644(-5)	8.643(-5)	8.641(-5)

the boundary condition was $\phi_{,\mathbf{n}} = 1$ on both sides and calculations with wave numbers $k = 1, 2, 3$ were carried out. The L_2 norms for the differences in the potential solutions for the $+$ side of the crack were $8.112982(-5)$, $1.475094(-4)$ and $1.636466(-4)$ for the three wave numbers, respectively. For the $-$ side, the results were nearly the same, $8.111455(-5)$, $1.474268(-4)$ and $1.636228(-4)$. As the potentials on both sides (for the disk problem as well) agree, the jump in potentials also agree. Employing just the hypersingular equation to compute $[\phi]$ is therefore completely consistent with an algorithm that depends upon both equations.

5 Conclusion

A linear element Galerkin approximation of the potential and velocity boundary integral equations for the 3D Helmholtz equation has been reported. The singular integrations are based upon a direct limit evaluation, and the required analytic integrations are made possible by invoking a two-term Taylor series expansion of the exponential e^{ikr}. Although the linear element is also key to being able to evaluate the integrals analytically, the techniques are not limited to this approximation; the exact integrations and limit analysis for a higher order interpolation can be based upon the linear element analysis.

The (derivative) velocity equation plays a key role in handling irregular frequencies, and thus it is important to note that the Galerkin form, together with the limit definition, allow a direct treatment of this equation. Although components of the hypersingular integral are divergent (coincident and edge-adjacent integrals), the complete integral is finite and can be evaluated without regularization, reformulation, or finite part analysis. Moreover, as the limit algorithm is the same irrespective of the order of the singularity, it is not necessary to have different evaluation schemes for the different kernel functions .

Two standard boundary integral methods for treating a fracture geometry, a dual equation approach (potential and velocity equations) and a hypersingular-only for-

mulation have been developed. The two methods produced essentially the same results for all test problems, providing a strong indication that both equations have been implemented correctly.

References

Bonnet, M.; Maier, G.; Polizzotto, C. (1998):   Symmetric Galerkin boundary element method. *ASME Appl. Mech. Rev.*, vol. 51, no. 11, pp. 669–704.

Bui, H. D. (1977):   An integral equation method for solving the problem of a plane crack of arbitrary shape. *J. Mech. Phys. Solids*, vol. 25, pp. 29–39.

Burton, A. J.; Miller, G. F. (1971):   The application of integral equation methods for the numerical solution of boundary value problems. *Proc. Roy. Soc. London*, vol. A232, pp. 201–210.

Chien, C. C.; Rajiyah, H.; Atluri, S. N. (1990):   An effective method for solving the hypersingular integral equations in 3-D acoustics. *J. Acoustic Soc. Am.*, vol. 88, no. 2, pp. 918–937.

Cruse, T. A. (1988):   *Boundary Element Analysis in Computational Fracture Mechanics*. Kluwer Academic Publishers, Boston.

Fata, S. N.; Gray, L. J. (2009):   Semi-analytic integration of hypersingular Galerkin BIEs for 3D potential problems. *J. Comput. Appl. Math.*, vol. 231, no. 2, pp. 561–576.

Frangi, A. (1998):   Regularization of boundary element formulations by the derivative transfer method. In Sladek, V.; Sladek, J.(Eds): *Singular Integrals in the Boundary Element Method*, Advances in Boundary Elements, chapter 4, pp. 125–164. Computational Mechanics Publishers.

Graciani, E.; Mantič, V.; Paris, F.; Cañas, J. (2000):   A critical study of hypersingular and strongly singular boundary integral representations of potential gradient. *Comp. Mech.*, vol. 25, pp. 542–559.

Gray, L. J. (1989):   Boundary element method for regions with thin internal cavities. *Engng. Analy. Boundary Elements*, vol. 6, pp. 180–184.

Gray, L. J.; Glaeser, J.; Kaplan, T. (2004): Direct evaluation of hypersingular Galerkin surface integrals. *SIAM J. Sci. Comput.*, vol. 25, no. 5, pp. 1534–1556.

Gray, L. J.; Phan, A.-V.; Kaplan, T. (2004): Boundary integral evaluation of surface derivatives. *SIAM J. Sci. Comput.*, vol. 26, no. 1, pp. 294–312.

Gray, L. J.; Salvadori, A.; Phan, A.-V.; Mantič, V. (2006): Direct evaluation of hypersingular Galerkin surface integrals II. *Elect. J. Boundary Elements*, vol. 4, no. 3, pp. 105–130.

Hong, H. K.; Chen, J. T. (1988): Derivation of integral equations in elasticity. *J. ASCE, Eng. Mech. Div.*, vol. 114, pp. 1028–1044.

Hwang, W. S. (1997): A boundary integral method for acoustic radiation and scattering. *J. Acoustic Soc. Am.*, vol. 101, pp. 3330–3335.

Hwang, W. S. (1997): Hypersingular boundary integral equations for exterior acoustic radiation problems. *J. Acoustic Soc. Am.*, vol. 101, pp. 3336–3342.

Ioakimidis, N. I. (1982): A natural approach to the introduction of finite-part integrals into crack problems of three-dimensional elasticity. *Engng. Fract. Mech.*, vol. 16, pp. 669–673.

Kleinman, R. E.; Roach, G. (1974): Boundary integral equations for the three-dimensional Helmholtz equation. *SIAM Rev.*, vol. 16, no. 2, pp. 214–236.

Maier, G.; Novati, G.; Cen, Z. (1995): Symmetric-galerkin boundary element method for quasi-brittle fracture and frictional contact problems. *Comp. Mech.*, vol. 17, pp. 74–89.

Martin, P. A. (2006): *Multiple Scattering*. Cambridge University Press, Cambridge.

Martin, P. A.; Rizzo, F. J. (1989): On boundary integral equations for crack problems. *Proc. R. Soc. Lond.*, vol. A421, pp. 341–355.

Okada, H.; Rajiyah, H.; Atluri, S. N. (1989): Non-hypersingular integral representations for velocity (displacement) gradients in elastic/plastic solids (small or finite deformations). *Comp. Mech.*, vol. 4, pp. 165–175.

Polimeridis, A. G.; Yioultsis, T. V. (2008): On the direct evaluation of weakly singular integrals in galerkin mixed potential integral equation formulations. *IEEE Transactions on Antennas and Propagation*, vol. 56, pp. 3011–3019.

Portela, A. (1993): *Dual Boundary Element Analysis of Crack Growth*. Computational Mechanics Publications, Southampton.

Qian, Z. Y.; Han, Z. D.; Atluri, S. N. (2004): Directly derived Non-Hyper-Singular boundary integral equations for acoustic problems, and their solution

through Petrov-Galerkin schemes. *CMES: Computer Modeling in Engineering & Sciences*, vol. 5, no. 6, pp. 541–562.

Qian, Z. Y.; Han, Z. D.; Ufimtsev, P.; Atluri, S. N. (2004): Non-Hyper-Singular boundary integral equations for acoustic problems, implemented by the collocation based boundary element method. *CMES: Computer Modeling in Engineering & Sciences*, vol. 6, no. 2, pp. 133–144.

Schwab, C.; Wendland, W. L. (1999): On the extraction technique in boundary integral equations. *Math. Comp.*, vol. 68, no. 225, pp. 91–122.

Sutradhar, A.; Paulino, G. H.; Gray, L. J. (2008): *Symmetric Galerkin Boundary Element Method*. Springer-Verlag, Berlin.

von Estorff, O.; Rjasanow, S.; Stolper, M.; Zaleski, O. (2005): Two efficient methods for a multifrequency solution of the Helmholtz equation. *Comput. Vis. Sci.*, vol. 8, no. 3-4, pp. 159–167.

Wu, T. W.; Seybert, A. F.; Wan, G. C. (1991): On the numerical implementation of a Cauchy principal integral to insure a unique solution for acoustic radiation and scattering. *J. Acoustic Soc. Am.*, vol. 90, pp. 554–560.

Wu, T. W.; Wan, G. C. (1992): Numerical modeling of acoustic radiation and scattering from thin bodies using a Cauchy principal integral equation. *J. Acoustic Soc. Am.*, vol. 92, pp. 2900–2906.

Yang, S. A. (2000): An investigation into integral equation methods involving nearly singular kernels for acoustic scattering. *J. Sound and Vibration*, vol. 234, pp. 225–239.

Zhao, Z. Y.; Lan, S. (1999): Boundary stress calculation - a comparison study. *Computers and Structures*, vol. 71, no. 1, pp. 77–85.